Journal of Zhejiang University-SCIENCE A (Applied Physics & Engineering)
ISSN 1673-565X (Print); ISSN 1862-1775 (Online)
www.jzus.zju.edu.cn; www.springerlink.com
E-mail: jzus@zju.edu.cn

Effect of seal clearance on the separation performance for a gearbox sealing system of a high-speed electric multiple unit*

Yu ZHANG†, Kai-lin ZHANG, Yuan YAO

State Key Laboratory of Traction Power, Southwest Jiaotong University, Chengdu 610031, China

†E-mail: zhangyutpl@163.com

Received Jan. 3, 2019; Revision accepted Apr. 26, 2019; Crosschecked Apr. 29, 2019

Abstract: Seal characteristic is based on the oil-gas separation performance of the gearbox sealing system of a high-speed electric multiple unit. A model of the gearbox sealing system is established to study the effect of seal clearance on separation performance, based on discrete phase method and droplet-wall collision models. The results show that the airflow drag force and oil droplet inertia force affect the locus of the droplet motion and the oil-gas separation efficiency of the sealing system. However, mass inertia force is the major influencing factor while acceleration inertia force and airflow drag force are secondary factors. The separation efficiency of small oil droplet (diameter 1 μm) decreases as the axial clearance width increases, while the separation efficiency of larger oil droplet (diameter 5 μm) remains unchanged. However, the separation efficiency of intermediate droplet (diameter 2−4 μm) decreases and then increases. Meanwhile, larger axial clearance height difference and radial tooth relative meshing ratio lead to higher separation efficiency. The separation efficiency decreases with increasing radial tooth angle, reaches a minimum at 80°, and then increases with further increase in tooth angle. Thus, the seal clearance has a slight effect on the oil-gas separation efficiency of oil droplet of 5 μm.

Key words: Gearbox sealing system; Seal clearance; Separation performance; Discrete phase method (DPM) model; Droplet-wall collision model

https://doi.org/10.1631/jzus.A1900004 **CLC number:** TH113

1 Introduction

Gearbox is an important component of the driving system of high-speed electric multiple unit (EMU), whose performance directly determines the safety of train operation. To ensure the lubrication and cooling of the high-speed gearbox, some lubrication oil is required to maintain in the gearbox interior and a complicated sealing system is set. Meanwhile, the gearbox sealing system usually adopts non-contact labyrinth sealing to avoid structural wear caused by sealing materials, thereby lengthening the lifetime of the equipment.

Non-contact labyrinth sealing reduces leakage by generating high flow resistance in the sealing medium through a complex fluid flow. Meanwhile, straight-through labyrinth seal has been widely used in rotating machineries as a typical non-contact labyrinth seal. However, it has serious ventilation effects which results in low sealing efficiency. Thus, a large number of sealing teeth is required to obtain a high sealing efficiency (Feng et al., 2018). Furthermore, the sealing structure needs to be optimized if it has a limited space such that the number of sealing teeth cannot be guaranteed. Hence, interlacing (He et al., 2015) and stepped (Tong and Cha, 2009) labyrinth seals have been widely applied in this case by changing the relative position of the sealing teeth to

* Project supported by the National Natural Science Foundation of China (Nos. 51675443 and 51735012) and the Independent Research and Development Projects of State Key Laboratory of Traction Power, Southwest Jiaotong University, China (Nos. 2017TPL_T02 and 2018TPL_T05)

ORCID: Yu ZHANG, https://orcid.org/0000-0003-0710-5828

obliterate the ventilation effect. Several studies have illustrated that the sealing efficiency of the interlacing and stepped labyrinth seals can be improved by over 30% in comparison with the straight-through seal. Alizadeh et al. (2018) compared the sealing performance of honeycomb labyrinth seal with stepped labyrinth seal and pointed out that seal clearance width is the key factor in determining the sealing performance. During the operation of the sealing system, the seal clearance width is altered due to the wear of the tooth tip area (Dogu et al., 2016), and centrifugal and thermal deformations (Subramanian et al., 2015, 2016), thereby affecting the labyrinth sealing performance.

The previous studies often used ideal gas as a medium and analyzed the sealing performance based on energy dissipation principle. However, the media inside the gearbox is a mixture of lubricating oil and gas. The pressure difference force derived from the high pressure inside the gearbox and the negative pressure outside the gearbox causes media leakage. The lubricating oil leakage in the sealing system is reduced by balancing the pressure inside and outside the gearbox. Hence, it is necessary to study the gas-oil separation efficiency of the gearbox sealing system, to analyze the sealing performance. The separated lubricating oil returns to the gearbox interior through the oil return structure, thereby improving the sealing performance. Therefore, oil return facilitates oil-gas separation, and the study of the separation characteristics is important for analyzing the sealing performance of the gearbox sealing system.

Guizani et al. (2017) found that the flow field enhanced the understanding of the separation mechanisms, although it was difficult to obtain flow field detail by experimental tests. The flow field in the separator is obtained by numerical simulation and further validated by comparison with experimental results. Elsayed and Lacor (2010) and Safikhani et al. (2010) analyzed the effect of inlet structure on the separation efficiency of cyclone separators, based on discrete phase method (DPM) model. They found that the inlet structure determined the pre-whirl angle and inlet velocity of gas and particles. Meanwhile, Elsayed and Lacor (2011), Gao et al. (2014), and Elsayed (2015) studied the influences of the outlet diameter and center channel of the cyclone separator on the separation efficiency. They found that the cone was an essential part of the cyclone separator that was beneficial for the particle separation, and that the outlet diameter of the cyclone separator had a slight effect on the separation efficiency. However, they assumed that the oil droplet stuck with wall surface after collision, thereby accounting for the high separation efficiency obtained in the numerical simulation. On the other hand, Wen et al. (2016) analyzed the effect of internal clearance width induced by delta wing structure on the gas flow and particle trajectories of a supersonic separator. The separation mechanism of a supersonic separator was determined by considering the droplets that rebounded or stuck with the wall after collision. Based on the previous research and the supersonic separator structure, Liu et al. (2014) determined the influence of liquid properties and swirl conditions on gas-water separation efficiency by comparing the numerical simulation with experimental test. They found that the numerical conclusions were consistent with the experimental results. Therefore, this paper adopts the droplet-wall collision model and oil-gas mixture as a working media to achieve a reliable simulation result.

In this paper, the gearbox sealing system of high-speed EMU is taken as research object. Based on the concept of oil-gas separation and the DPM and droplet-wall collision models, the separation mechanism of the sealing system is explored and the effect of seal clearance on separation efficiency is analyzed by Fluent software. This study provides theoretical basis for optimizing the structure parameters to improve the separation and sealing performance of gearbox sealing systems.

2 Physical model

The structural scheme of the gearbox sealing system of high-speed EMU is shown in Fig. 1. The sealing system consists of sealing and oil return structures. Meanwhile, the sealing structure comprises an axial bilateral straight-through labyrinth seal and a radial plug-in labyrinth seal. In the axial labyrinth seal, the rotor and stator structures are made up of three cavities (I−III) and an axial clearance which exists between the cavities. On the other hand, the radial seal is formed by the insertion of sealing teeth and the radial clearance is determined by different tooth angles and relative meshing depths.

The oil return structure is set at the bottom of the sealing structure (Fig. 1a). When the oil droplets collide with the wall surface of the sealing structure, some droplets adhere to the wall surface and flow to the oil return structure under the influence of gravitational force. Due to the differential pressure between the inlet pressure of the sealing structure and the outlet pressure of the oil return structure, the oil returns to the gearbox interior, thereby recovering the oil and reducing its leakage.

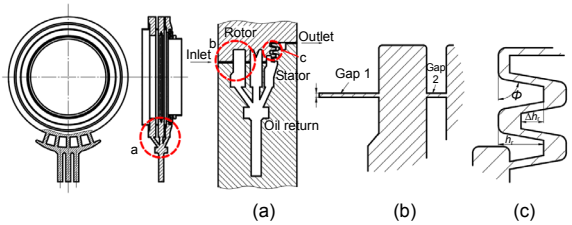

Fig. 1 Structural scheme of sealing system: (a) oil return structure; (b) axial seal; (c) radial seal

Fig. 1b shows the axial seal whose flow field is influenced by the axial clearance width c and the clearance height difference Δh. Δh is the height difference between the inlet clearance (gap 1) and the clearance (gap 2) between cavities I and II, which is zero in Fig. 1. Moreover, Fig. 1c shows the radial seal. The radial clearance width and cavity space on the top of the tooth are determined by the radial tooth angle Φ and the relative meshing ratio η:

$$\eta=\Delta h_r/h_r, \tag{1}$$

where h_r is the radial sealing tooth height and Δh_r is the sealing tooth meshing height.

The initial axial clearance width of the sealing structure is 1 mm, Δh=0, Φ=80°, and η=0.5. The change of clearance width due to wear, temperature, and centrifugal deformation is not considered in this study.

3 Mathematical model

The flow field of the oil-gas medium in the gearbox sealing system has many complex unsteady vortices. However, Reynolds stress model (RSM) and renormalization group (RNG) k–ε models are often used to solve these problems. Meanwhile, RSM model is more accurate but has a low efficiency. Although RNG k–ε model is less accurate than the RSM model, it can meet the requirements of the complex structure. Thus, RNG k–ε model has been generally used in engineering applications (Karagoz and Kaya, 2007).

3.1 DPM model

The number of oil droplets in the gearbox sealing system is usually low while the volume fraction of oil droplets is usually less than 10%. The droplet was considered as a spherical particle while DPM model was used to track the locus of the oil droplet motion. Meanwhile, gas is a continuous phase while oil droplet is a discrete phase. Thus, the interaction between discrete and continuous phases, and the Saffman lift force were considered.

In the Cartesian coordinate system, the discrete phase equilibrium differential equation (Gao et al., 2013) is given by

$$\frac{\mathrm{d}u_p}{\mathrm{d}t}=F_D(u-u_p)+\frac{g(\rho_p-\rho)}{\rho_p}+F_{saf}, \tag{2}$$

$$F_D=\frac{18\mu}{\rho_p d_p^2}\frac{C_D Re}{24}, \tag{3}$$

$$Re=\frac{\rho d_p\left|u_p-u\right|}{\mu}, \tag{4}$$

$$C_D=a_1+\frac{a_2}{Re}+\frac{a_3}{Re^2}, \tag{5}$$

where u and u_p are the continuous and discrete phase velocities, respectively; ρ and ρ_p are the continuous and discrete phase densities, respectively; μ is the continuous phase viscosity, d_p is the discrete phase diameter, F_D is the drag force under the unit particle mass, F_{saf} is the Saffman lift force, C_D is the drag coefficient, a_1, a_2, and a_3 are constants, Re is the discrete phase Reynolds number, t is the time, and g is the gravitational acceleration.

The velocity of discrete phases at any position can be obtained using Eqs. (3)–(5) while the motion trajectories of the particles can be tracked by integrating u_p.

3.2 Droplet-wall collision model

The oil droplet may rebound, spread, and splash when it collides with the wall surface, as shown in Fig. 2. During the collision process, the energy and

velocity of the droplet change. The variation in the velocity of the oil droplet depends on the physical parameters, incident angle, incident velocity of the oil, and the characteristics of the wall surface.

The state of the oil droplet is determined by the Weber number and Laplace number (Bai and Gosman, 1995) after the collision. The Weber number is the ratio of the inertial force to the surface tension while Laplace number is the ratio of the surface tension to the viscous force:

$$We=\frac{\rho_{\mathrm{p}}V_{\mathrm{n}}^{2}d_{\mathrm{p}}}{\sigma}, \tag{6}$$

$$La=\frac{\rho_{\mathrm{p}}\sigma d_{\mathrm{p}}}{\mu_{\mathrm{p}}^{2}}, \tag{7}$$

where σ is the surface tension of oil droplet , V_{n} is the normal collision velocity of oil droplet, and μ_{p} is the viscosity of oil droplet.

For a rebounding droplet, the velocity-rebound coefficient e is the ratio of the rebound velocity to the initial velocity of oil droplets, which is determined by the incident angle, and described in Eqs. (8) and (9) (Grant and Tabakoff, 1975).

$$e_{\mathrm{n}}=0.993-0.176\theta+1.56\theta^{2}-0.49\theta^{3}, \tag{8}$$

$$e_{\tau}=0.988-1.66\theta+2.11\theta^{2}-0.67\theta^{3}, \tag{9}$$

where e_{n} and e_{τ} are the rebound coefficients in the normal and tangential directions, respectively; θ is the incident angle.

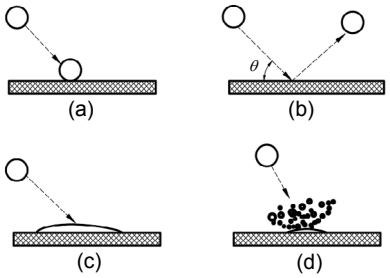

Fig. 2 Schematic diagram of the collision between an oil droplet and wall surface
(a) Stick; (b) Rebound; (c) Spread; (d) Splash

Meanwhile, the state of the oil droplet after collision changes based on the increase of the Weber number, as follows:

Stick→Rebound→Spread→Splash.
Stick→Rebound:

$$We_{\mathrm{c}}\approx 1; \tag{10}$$

Rebound→Spread:

$$We_{\mathrm{c}}\approx 5; \tag{11}$$

Spread→Splash:

$$We_{\mathrm{c}}=1320La^{-0.18}, \tag{12}$$

where We_{c} is the critical value of Weber number between the different oil droplets conditions after collision. During the analysis of gearbox sealing system, the oil droplets will not splash due to large We_{c}. Thus, the wall surface is considered wet when the collision between the oil droplets and wall surface is studied.

3.3 Boundary conditions

The pressure boundary condition of the oil-gas flow field is set at the inlet and outlet of the gearbox sealing system. The inlet and outlet pressures of the sealing structure are 500 Pa and −700 Pa, respectively. However, the outlet pressure of the oil return structure is dependent on the internal pressure of the gearbox oil pool and is set at 200 Pa. The rotor speed is set at 3000 r/min. Moreover, 75W_90 grade lubrication oil with density of 843 kg/m^3 and viscosity of 16.6 mm^2/s is used in the gearbox. In the simulation, the oil droplet diameter D is set in the range of 1–5 μm.

Furthermore, the escape condition of the oil droplet motion is set at the inlet and outlet of the sealing system. However, the oil droplets which escaped from the inlet and outlet sections are excluded in the next calculation. Meanwhile, a user defined function is adopted for the wall surface of the sealing system. Based on the collision condition and droplet-wall collision model, DEFINE_DPM_BC is compiled in the Fluent software. When the Weber number of the incident oil droplets ranges from 1 to 5, the oil droplets rebound according to Eqs. (8) and (9), and then return to the flow field in the next calculation. However, when the Weber number of the incident oil droplets is less than 1 or greater than 5, the oil droplets adhere to the wall surface and are thus removed from the next calculation.

The oil-gas separation efficiency of gearbox sealing system is calculated by

$$\eta_{\text{sep}} = \left(1 - \frac{m_{\text{outescape}}}{m_{\text{all}}}\right) \times 100\%, \tag{13}$$

where $m_{\text{outescape}}$ and m_{all} are the oil droplets mass at the sealing structure inlet and outlet, respectively.

3.4 Experimental validation

The labyrinth-type separator with baffle (LTB) in diesel engine valve chamber cover was numerically analyzed and the oil-gas separation efficiency with oil droplets of different diameters was calculated, to verify the accuracy of DPM and droplet-wall collision models. An oil-gas separation efficiency test bench was used to obtain the mass of oil droplet at the inlet and outlet of the cover per unit time. The separation efficiency is the ratio of collected oil droplet mass relative to the original mass. The details of LTB structure and boundary conditions are described by Zhang (2014).

Table 1 summarizes the separation efficiencies obtained by numerical calculations and experimental tests for different droplet diameters. The maximum deviation is less than 5%, indicating that the results are reliable and DPM and droplet-wall collision models are suitable for the flow field analysis of a labyrinth separator.

Table 1 Oil-gas separation efficiency

Oil diameter (μm)	Simulation result (%)	Test result (%)	Error (%)
3	64.8	68	3.2
5	69.1	72	2.9
10	73.9	78	4.1

4 Results and discussion

4.1 Mesh sensitivity analysis

The density and quality of the grid system are of great importance in simulation accuracy and efficiency. In the gearbox sealing system, the mesh was generated using an unstructured mesh and some key areas such as seal clearance were partially refined. Five grids with different densities were employed to study the grid independence, with the cell number ranging from 0.5 million to 1.8 million, while outlet gas flow was used as the characteristic parameter. Fig. 3 shows the mesh independence for the simulation model. The outlet gas flow decreases with an increase in cell number. If the cell number is further increased, the outlet gas flow tends to be stable, and the grid density has only a slight effect on the outlet gas flow. A discrete model with 1.53 million grids was selected for the subsequent simulation, based on the calculation accuracy and efficiency.

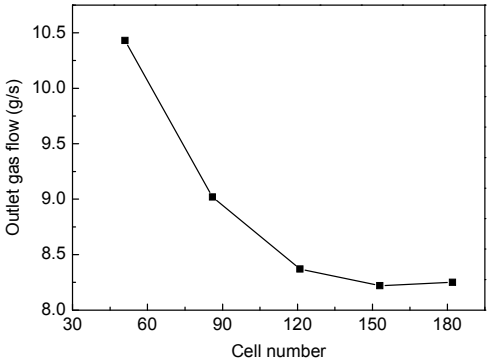

Fig. 3 Mesh independence for the simulation model

4.2 Effect of axial clearance width

The axial clearance width influences the flow field distribution and the locus of the oil droplet motion in the sealing system, and further impacts the oil-gas separation efficiency. The separation efficiency of the gearbox sealing system was calculated for an axial clearance width ranging from 0.5 mm to 1.8 mm with other boundary conditions unchanged, to study the influence of the axial clearance width on the separation performance. Fig. 4 shows the effect of axial clearance width on oil-gas separation efficiency and outlet gas flow for different droplet diameters.

The separation efficiency decreases with increase in axial clearance width for small oil droplet under a constant oil droplet (D=1 μm), and has a slight effect on the large oil droplet (D=5 μm). For oil droplets of 2–4 μm diameter, the separation efficiency decreases and then increases with increasing axial clearance width. As the oil droplet diameter increases, the inflexion point of axial clearance width corresponding to the lowest separation efficiency decreases. Hence, an increase in the oil droplet diameter enhances the oil-gas separation and weakens the effect of axial clearance width on separation efficiency. Moreover, the diameter of oil droplets plays an

increasingly important role in oil-gas separation while the outlet gas flow increases as the axial clearance width increases.

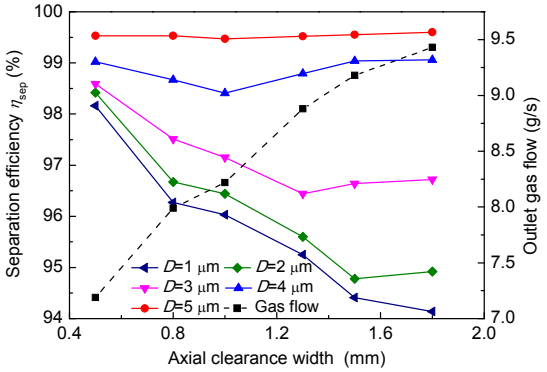

Fig. 4 Effect of axial clearance width on separation efficiency and outlet gas flow

However, the oil droplets in the flow field of the gearbox sealing system were subjected to airflow drag force and inertial force. The inertial force of oil droplets is determined by the mass and acceleration, which are defined as mass inertial force and acceleration inertial force, respectively. For oil droplets with larger diameters, the mass inertia force was reinforced. When an oil droplet moves, the variations in velocity magnitude and direction enhance the acceleration inertia force due to sealing structural restriction. Thus, the oil droplet withstands airflow and the airflow drag force.

The strong inertial force and weak drag force lead to higher separation efficiency. However, the mass inertia force majorly affects the oil-gas separation efficiency while acceleration inertia force and airflow drag force are secondary factors. Therefore, the diameter of oil droplet is essential for enhancing separation efficiency for a large seal clearance width.

Fig. 5 shows the trajectory of oil droplets (1 μm) under different axial clearance widths. The mass inertia force of oil droplets with small diameter (1 μm) is small. However, the separation probability of oil droplets in the cavities and the incident velocity decrease as the axial clearance width increases. When the small oil droplets swirl with the gas in the cavities, the acceleration inertia force keeping the oil droplets in motion state weakens. Thus, the flow of the oil droplets with the gas becomes easier. This leads to a reduced probability of collision of the oil droplets with the wall surface, thereby decreasing the oil-gas separation efficiency. Thus, more oil droplets can move into the cavities as the axial clearance width becomes wider. Meanwhile, the incident velocity of airflow and the airflow drag force decrease, leading to an increase in the oil-gas separation efficiency. However, the acceleration inertia force plays a more important role in comparison with the airflow drag force. Hence, the separation efficiency of a small oil droplet decreases with increasing clearance width while the decreased degree of separation efficiency decreases.

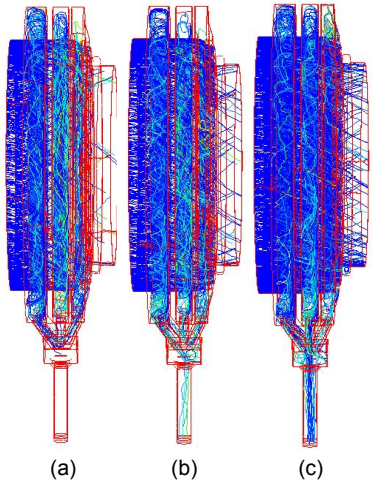

Fig. 5 Trajectory of oil droplets (1 μm) under different axial clearance widths
(a) 0.5 mm; (b) 1.0 mm; (c) 1.8 mm

For oil droplets with large diameter (5 μm), the mass inertia force plays a major role, while the acceleration inertia force and airflow drag force which are determined by the sealing system structure have limited impact on the motion state of the oil droplets and the oil-gas separation efficiency. Therefore, the change in axial clearance width has a slight impact on the separation efficiency.

However, the mass inertia force of an oil droplet with a fixed intermediate diameter (2–4 μm) is constant. Meanwhile, the acceleration inertia force of oil droplets weakens as the axial clearance width increases, thereby leading to a decrease in the oil-gas separation efficiency. Furthermore, the airflow drag force becomes strong, thereby leading to an increase in the oil-gas separation efficiency. However, the acceleration inertia force is greater than the airflow

drag force and mass inertia force when the axial clearance width is small. This results in a decrease in the oil-gas separation efficiency as the axial clearance width increases. Furthermore, the acceleration inertia force is equal to the airflow drag force and mass inertia force when the axial clearance width increases to a certain value (W_{ip}), such that the oil-gas separation efficiency reaches a minimum. When the clearance width continues to increase, the acceleration inertia force is weaker than the airflow drag force and mass inertia force, thereby leading to an increase in the oil-gas separation efficiency as the axial clearance width increases. The observations made above are reasonable. On the other hand, the mass inertia force strengthens as the oil droplet diameter increases. Furthermore, the oil-gas separation efficiency approaches its minimum value when the acceleration inertia force is equal to the airflow drag force and mass inertia force. For large oil droplets with relatively strong mass inertia force, the lowest separation efficiency is obtained when the decreased degree of the acceleration inertia force decreases. Thus, the increasing range of clearance width reduces. Hence, the inflexion point of axial clearance width (W_{ip}) corresponding to the lowest separation efficiency decreases as the oil droplet diameter increases.

4.3 Effect of axial clearance height difference

When the axial clearance height in the sealing system is unequal, the straight passage of the clearance is disrupted and a stepped passage is formed, which affects the flow field distribution and changes the oil-gas separation efficiency. The separation efficiency of the gearbox sealing system was calculated for an axial clearance height difference ranging from −4 mm to 4 mm with other boundary conditions unchanged, to study the effect of axial clearance height on separation performance. Fig. 6 shows the effect of axial clearance height difference on oil-gas separation efficiency and outlet gas flow under different droplet diameters.

The oil-gas separation efficiency increases with axial clearance height difference under constant oil droplet diameter, while the separation efficiency curve is symmetrical with respect to zero axial clearance high difference. Meanwhile, the oil-gas separation efficiency shows an increased trend with increasing diameter of the oil droplet. However, the axial clearance height has less significant effect on the separation efficiency than the axial clearance width. Moreover, the outlet gas flow increases and reaches a maximum at zero axial clearance high difference as the height difference absolute value decreases.

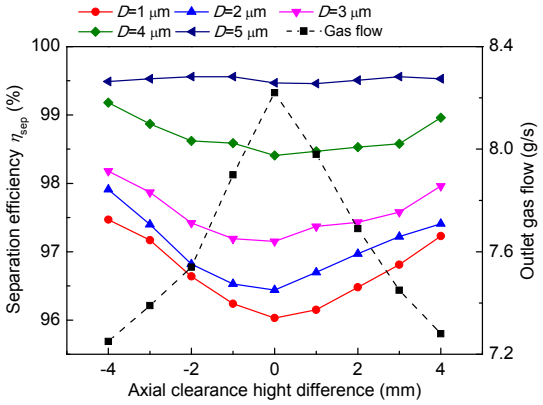

Fig. 6 Effect of axial clearance height difference on separation efficiency and outlet gas flow

Under constant oil droplet diameter, a larger axial clearance height difference significantly disrupts the straight passage, which explains the decrease in outlet gas flow. When the axial clearance height difference is larger, the proportion of oil droplets flow into the cavities increases. Thus, a strong vortex is formed in the cavities due to the structure restriction. It can then be assumed that the oil droplet motion locus becomes more complex, thereby facilitating collisions between oil droplets and the wall surface. Thus, more oil droplets can be captured by the wall surface, leading to an increase in the oil-gas separation efficiency. When the absolute value of axial clearance height difference is uniform, its influence on the flow field and separation efficiency is similar as the stepped passage is symmetrical.

Thus, mass inertia force significantly affects oil-gas separation as the oil droplet diameter increases, thereby sustaining the original motion state of the oil droplets. Meanwhile, the axial clearance height difference is less significant. For an oil droplet with diameter over 5 μm, the influence of axial clearance height difference on oil-gas separation efficiency is nearly insignificant.

4.4 Effect of radial tooth angle

The radial sealing tooth angle is limited by the structural space of the sealing system. However,

various radial clearance widths were formed by the meshing of radial teeth at different angles, thereby affecting the flow field and oil-gas separation efficiency. Thus, the separation efficiency of the gearbox sealing system was calculated for Φ ranging from 70° to 90° with other boundary conditions unchanged, to analyze the influence of Φ on separation performance. Fig. 7 shows the effect of Φ on the oil-gas separation efficiency and outlet gas flow under different droplet diameters.

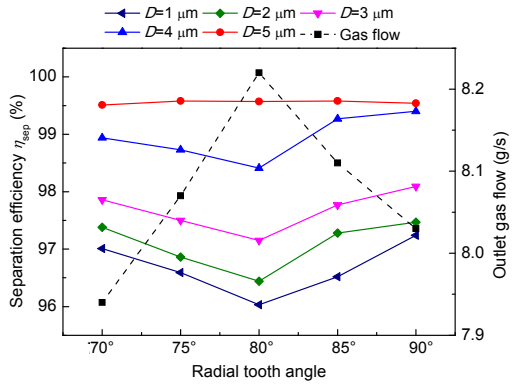

Fig. 7 Effect of radial tooth angle on separation efficiency and outlet gas flow

The oil-gas separation efficiency decreases and then increases as Φ is increased, under constant oil droplet diameter. When Φ is 80°, the oil-gas separation efficiency is the lowest while the outlet gas flow is the largest. Furthermore, the influence of Φ on separation efficiency becomes weaker as the oil droplet diameter increases. Meanwhile, the influence of Φ on separation efficiency is insignificant for an oil droplet with diameter over 5 μm.

The radial airflow passage is determined by Φ, which affects the airflow drag force of oil droplets. When Φ is 80°, a high-speed airflow passage is formed, which is similar to the straight passage of straight-through labyrinth seal. Since the airflow drag force is strong and the oil droplet escape passage is smooth, the oil droplets wrapped in the airflow quickly pass through the radial sealing region, thereby decreasing the oil-gas separation efficiency. When Φ is not 80°, the high-speed passage is disrupted while the airflow drag force is weak, thereby leading to an increase in the oil-gas separation efficiency. Meanwhile, the mass inertia force significantly influences the separation efficiency as the oil droplet diameter increases. However, the mass inertia force of the oil droplet of diameter 5 μm plays a major role while the acceleration inertia force and airflow drag force play minor roles. Therefore, the separation efficiency is not affected by Φ.

4.5 Effect of radial meshing ratio

The clearance is formed by the radial teeth in the plug-in labyrinth seal. However, the relative meshing depth of the radial seal tooth determines the radial clearance width, which further affects the oil-gas separation efficiency. To analyze the influence of η on the separation performance, the separation efficiency of the gearbox sealing system was calculated for η ranging from −0.1 to 0.9 with other boundary conditions unchanged. Fig. 8 shows the effect of η on oil-gas separation efficiency and outlet gas flow under different droplet diameters.

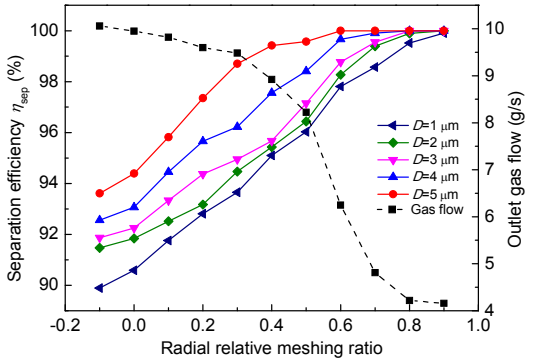

Fig. 8 Effect of radial relative meshing ratio on separation efficiency and outlet gas flow

Under constant oil droplet diameter, the oil-gas separation efficiency increases as η increases such that oil-gas separation is achieved. Meanwhile, the oil-gas separation efficiency increases as the oil droplet diameter increases, thereby leading to a decrease in η which indicates complete separation. The outlet gas flow decreases with η and then stabilizes.

Meanwhile, the radial sealing flow passage becomes complex as η increases, under constant oil droplet diameter; while the cavity space at the top of sealing tooth reduces. When the oil droplets pass through the complex flow passage, their speed magnitude and direction change, thereby leading to an enhancement of the acceleration inertia force. Consequently, the acceleration inertia force overcomes airflow drag force and increases the probability of

collision of oil droplets with the wall surface, thereby improving the oil-gas separation efficiency. When η is significantly large, the clearance width is small, causing the outlet gas flow to decrease, finally tending to a stable value. As a result, the small radial clearance width hinders the escape of oil droplets such that the oil and gas are completely separated. As the oil droplet diameter increases, the mass inertia force becomes more significant, which is favorable for the separation of the oil and gas. Therefore, the η corresponding to complete separation decreases.

5 Conclusions

Oil return is based on oil-gas separation whose characteristic determines the sealing performance of the gearbox sealing system of high-speed EMU. The effect of seal clearance on oil-gas separation efficiency under different droplet diameters was studied using DPM and droplet-wall collision models. The following conclusions are obtained:

1. Oil droplet inertia force and airflow drag force are the dominant factors affecting oil-gas separation. Stronger inertia force and weaker drag force lead to higher separation efficiency. Meanwhile, mass inertia force is the major factor, while acceleration inertia force and airflow drag force are the secondary factors.

2. As the axial clearance width increases, the separation efficiency of small oil droplets (1 μm) decreases, while the separation distance of large droplets (5 μm) remains unchanged. Meanwhile, the separation efficiency of intermediate droplets (2–4 μm) decreases and then increases. The increase in the axial clearance height difference enhances the oil-gas separation efficiency.

3. As Φ increases, the oil-gas separation efficiency decreases and then increases, while the separation efficiency is the lowest when Φ is 80°. On the other hand, the oil-gas separation efficiency increases as η increases such that the oil and gas are completely separated.

4. The influence of seal clearance on separation efficiency becomes weaker as the oil droplet diameter becomes larger.

In summary, our research is beneficial to the design of gearbox sealing systems. However, the effect of oil droplet diameter and seal clearance (axial clearance width, axial clearance height difference, Φ and η) on oil-gas separation efficiency needs to be carefully considered during the design.

References

Alizadeh M, Nikkhahi B, Farahani AS, et al., 2018. Numerical study on the effect of geometrical parameters on the labyrinth–honeycomb seal performance. *Proceedings of the Institution of Mechanical Engineers, Part G: Journal of Aerospace Engineering*, 232(2):362-373. https://doi.org/10.1177/0954410017742227

Bai CX, Gosman AD, 1995. Development of Methodology for Spray Impingement Simulation. Technical Report No. 950283, SAE International, USA. https://doi.org/10.4271/950283

Dogu Y, Sertçakan MC, Bahar AS, et al., 2016. Computational fluid dynamics investigation of labyrinth seal leakage performance depending on mushroom-shaped tooth wear. *Journal of Engineering for Gas Turbines and Power*, 138(3):032503. https://doi.org/10.1115/1.4031369

Elsayed K, 2015. Optimization of the cyclone separator geometry for minimum pressure drop using Co-Kriging. *Powder Technology*, 269(6):409-424. https://doi.org/10.1016/j.powtec.2014.09.038

Elsayed K, Lacor C, 2010. Optimization of the cyclone separator geometry for minimum pressure drop using mathematical models and CFD simulations. *Chemical Engineering Science*, 65(22):6048-6058. https://doi.org/10.1016/j.ces.2010.08.042

Elsayed K, Lacor C, 2011. Numerical modeling of the flow field and performance in cyclones of different cone-tip diameters. *Computers & Fluids*, 51(1):48-59. https://doi.org/10.1016/j.compfluid.2011.07.010

Feng JM, Wang LZ, Yang H, et al., 2018. Numerical investigation on the effects of structural parameters of labyrinth cavity on sealing performance. *Mathematical Problems in Engineering*, 2018:5273582. https://doi.org/10.1155/2018/5273582

Gao X, Chen JF, Feng JM, et al., 2013. Numerical and experimental investigations of the effects of the breakup of oil droplets on the performance of oil-gas cyclone separators in oil-injected compressor systems. *International Journal of Refrigeration*, 36(7):1894-1904. https://doi.org/10.1016/j.ijrefrig.2013.06.004

Gao X, Chen JF, Feng JM, et al., 2014. Numerical investigation of the effects of the central channel on the flow field in an oil-gas cyclone separator. *Computers & Fluids*, 92: 45-55. https://doi.org/10.1016/j.compfluid.2013.11.001

Grant G, Tabakoff W, 1975. Erosion prediction in turbomachinery resulting from environmental solid particles. *Journal of Aircraft*, 12(5):471-478. https://doi.org/10.2514/3.59826

Guizani R, Mhiri H, Bournot P, 2017. Effects of the geometry of fine powder outlet on pressure drop and separation

performances for dynamic separators. *Powder Technology*, 314:599-607. https://doi.org/10.1016/j.powtec.2016.10.025

He WD, Wang C, Zhang YH, 2015. Study of the influence of labyrinth seal clearance on gearbox leakage with gas-fluid two-phase mixture. *Applied Mechanics and Materials*, 789-790:231-235. https://doi.org/10.4028/www.scientific.net/amm.789-790.231

Karagoz I, Kaya F, 2007. CFD investigation of the flow and heat transfer characteristics in a tangential inlet cyclone. *International Communications in Heat and Mass Transfer*, 34(9-10):1119-1126. https://doi.org/10.1016/j.icheatmasstransfer.2007.05.017

Liu XW, Liu ZL, Li YX, 2014. Investigation on separation efficiency in supersonic separator with gas-droplet flow based on DPM approach. *Separation Science and Technology*, 49(17):2603-2612. https://doi.org/10.1080/01496395.2014.938755

Safikhani H, Akhavan-Behabadi MA, Shams M, et al., 2010. Numerical simulation of flow field in three types of standard cyclone separators. *Advanced Powder Technology*, 21(4):435-442. https://doi.org/10.1016/j.apt.2010.01.002

Subramanian S, Sekhar AS, Prasad BVSSS, 2015. Influence of combined radial location and growth on the leakage performance of a rotating labyrinth gas turbine seal. *Journal of Mechanical Science and Technology*, 29(6):2535-2545. https://doi.org/10.1007/s12206-015-0545-8

Subramanian S, Sekhar AS, Prasad BVSSS, 2016. On the choice of initial clearance and prediction of leakage flow rate for a rotating gas turbine seal. *Proceedings of the Institution of Mechanical Engineers, Part C: Journal of Mechanical Engineering Science*, 230(10):1586-1601. https://doi.org/10.1177/0954406215581692

Tong SK, Cha KS, 2009. Comparative analysis of the influence of labyrinth seal configuration on leakage behavior. *Journal of Mechanical Science and Technology*, 23(10):2830-2838. https://doi.org/10.1007/s12206-009-0733-5

Wen C, Yang Y, Walther JH, et al., 2016. Effect of delta wing on the particle flow in a novel gas supersonic separator. *Powder Technology*, 304(12):261-267. https://doi.org/10.1016/j.powtec.2016.07.061

Zhang XJ, 2014. Analysis of plastic oil-gas separator for diesel engine valve chamber cover. *International Journal of Vehicle Structures & Systems*, 6(3):47-50. https://doi.org/10.4273/ijvss.6.3.01

中文概要

题　目：密封间隙对高速动车组齿轮箱密封系统分离性能的影响

目　的：研究高速动车组齿轮箱密封系统的密封性能的前提是分析内部油气分离性能。探讨密封系统中油气分离机理和密封间隙（轴向间隙宽度、轴向间隙高度差、径向密封齿形角和径向密封齿相对啮合深度）对油气分离效率的影响，为齿轮箱密封系统的优化设计提供理论基础。

创新点：1. 采用润滑油和空气混合介质作为工作介质，更贴合工程实践；2. 采用液滴-壁面碰撞模型，分析油气分离过程中液滴的运动状态。

方　法：1. 结合离散相模型和液滴-壁面碰撞模型，建立高速动车组齿轮箱的密封系统模型。2. 通过试验和数值计算对比，验证仿真模拟的准确性和模型的适用性。3. 通过仿真模拟，分析不同液滴直径下密封间隙对油气分离性能的影响；其中，密封间隙包含轴向间隙宽度、轴向间隙高度差、径向密封齿形角和径向密封齿相对插入深度比。

结　论：1. 气流对油滴的拖曳力和油滴的惯性作用影响油滴运动轨迹和密封系统的油气分离效率；其中质量惯性力是主要因素，加速度惯性力与气流拖曳力是次要因素。2. 随着轴向间隙宽度的增大，小直径油滴（1 μm）分离效率降低，大直径油滴（5 μm）分离效率基本不变，而过渡直径的油滴（2~4 μm）分离效率先降低后增高。3. 随着轴向间隙高度差和径向密封齿相对啮合深度的增大，油气分离效率增高。4. 随着径向密封齿形角的增大，油气分离效率先降低后升高，齿形角为 80° 时，分离效率最低。5. 油滴直径越大，密封间隙变化对油气分离效率的影响越小。

关键词：齿轮箱密封系统；密封间隙；分离性能；离散相模型；液滴-壁面碰撞模型